

Spin asymmetries for events with high p_T hadrons in DIS and an evaluation of the gluon polarization

B. Adeva,²⁰ E. Arik,² A. Arvidson,^{23,u} B. Badełek,^{23,25} G. Baum,¹ P. Berglund,⁸ L. Betev,^{13,o} R. Birsa,²² N. de Botton,¹⁹ F. Bradamante,²² A. Bravar,^{11,h} A. Bressan,²² S. Bültmann,^{1,v} E. Burtin,¹⁹ D. Crabb,²⁴ J. Cranshaw,^{18,b} T. Çuhadar,^{2,15} S. Dalla Torre,²² R. van Dantzig,¹⁵ B. Derro,⁴ A. Deshpande,^{26,ih} S. Dhawan,²⁶ C. Dulya,^{4,15,c} S. Eichblatt,^{18,d} D. Fasching,^{17,e} F. Feinstein,¹⁹ C. Fernandez,^{20,9} B. Frois,¹⁹ A. Gallas,²⁰ J. A. Garzon,^{20,9} H. Gilly,⁶ M. Giorgi,²² E. von Goeler,¹⁶ S. Goertz,³ G. Gracia,^{20,f} N. de Groot,^{15,g} M. Grosse Perdekamp,^{26,jh} K. Haft,¹³ D. von Harrach,¹¹ T. Hasegawa,^{14,i} P. Hautle,^{5,j} N. Hayashi,^{14,k} C. A. Heusch,^{5,l} N. Horikawa,¹⁴ V. W. Hughes,^{26,*} G. Igo,⁴ S. Ishimoto,^{14,m} T. Iwata,¹⁴ E. M. Kabuß,¹¹ A. Karev,¹⁰ H. J. Kessler,^{6,n} T. J. Ketel,¹⁵ J. Kiryluk,^{25,o} Yu. Kisselev,¹⁰ L. Klostermann,¹⁵ K. Kowalik,²⁵ A. Kotzinian,¹⁰ W. Kröger,^{5,l} F. Kunne,¹⁹ K. Kurek,²⁵ J. Kyyräinen,^{1,8} M. Lamanna,^{22,a} U. Landgraf,⁶ J. M. Le Goff,¹⁹ F. Lehar,¹⁹ A. de Lesquen,¹⁹ J. Lichtenstadt,²¹ M. Litmaath,^{15,a} A. Magnon,¹⁹ G. K. Mallot,^{11,a} F. Marie,¹⁹ A. Martin,²² J. Martino,^{19,y} T. Matsuda,^{14,i} B. Mayes,⁹ J. S. McCarthy,²⁴ K. Medved,¹⁰ W. Meyer,³ D. Miller,¹⁷ Y. Miyachi,¹⁴ K. Mori,¹⁴ J. Moromisato,¹⁶ J. Nassalski,²⁵ T. O. Niinikoski,⁵ J. E. J. Oberski,¹⁵ A. Ogawa,^{14,h} C. Ozben,^{2,x} H. Pereira,¹⁹ D. Peshekhonov,^{10,b} R. Piegaia,^{26,p} L. Pinsky,⁹ S. Platchkov,¹⁹ M. Plo,²⁰ D. Pose,¹⁰ H. Postma,¹⁵ J. Pretz,^{11,w} G. Rädcl,⁵ G. Reicherz,³ J. Roberts,⁹ M. Rodriguez,^{23,p} E. Rondio,²⁵ I. Sabo,²¹ J. Saborido,²⁰ A. Sandacz,²⁵ I. Savin,¹⁰ P. Schiavon,²² E. P. Sichtermann,^{15,26,z} F. Simeoni,²² G. I. Smirnov,¹⁰ A. Staude,¹³ A. Steinmetz,¹¹ U. Stiegler,⁵ H. Stuhmann,⁷ R. Sulej,^{25,r} F. Tassarotto,²² D. Thers,¹⁹ W. Tlaczala,^{25,r} A. Tripet,¹ G. Unel,² M. Velasco,¹⁷ J. Vogt,¹³ R. Voss,⁵ C. Whitten,⁴ R. Windmolders,^{12,w} R. Willumeit,⁷ W. Wiślicki,²⁵ A. Witzmann,^{6,s} A. M. Zanetti,²² K. Zaremba,^{25,r} and J. Zhao^{7,11}

(Spin Muon Collaboration)

¹Physics Department, University of Bielefeld, 33501 Bielefeld, Germany

²Bogaziçi University and Istanbul Technical University, Istanbul, Turkey

³Physics Department, University of Bochum, 44780 Bochum, Germany

⁴Department of Physics, University of California, Los Angeles, California 90024, USA

⁵CERN, 1211 Geneva 23, Switzerland

⁶Physics Department, University of Freiburg, 79104 Freiburg, Germany

⁷GKSS, 21494 Geesthacht, Germany

⁸Helsinki University of Technology, Low Temperature Laboratory and Institute of Particle Physics Technology, Espoo, Finland

⁹Department of Physics, and Institute for Beam Particle Dynamics, University of Houston, Houston, Texas 77204, USA

¹⁰JINR, Dubna, RU-141980 Dubna, Russia

¹¹University of Mainz, Institute for Nuclear Physics, 55099 Mainz, Germany

¹²University of Mons, Faculty of Science, 7000 Mons, Belgium

¹³Physics Department, University of Munich, 80799 Munich, Germany

¹⁴CIRSE and Department of Physics, Nagoya University, Furo-Cho, Chikusa-Ku, 464 Nagoya, Japan

¹⁵NIKHEF, Delft University of Technology, FOM and Free University, 1009 AJ Amsterdam, The Netherlands

¹⁶Department of Physics, Northeastern University, Boston, Massachusetts 02115, USA

¹⁷Department of Physics, Northwestern University, Evanston, Illinois 60208, USA

¹⁸Bonner Laboratory, Rice University, Houston, Texas 77251-1892, USA

¹⁹C.E.A. Saclay, DAPNIA, 91191 Gif-sur-Yvette, France

²⁰Department of Particle Physics, University of Santiago, 15706 Santiago de Compostela, Spain

²¹School of Physics, Tel Aviv University, 69978 Tel Aviv, Israel

²²Department of Physics, INFN Trieste and University of Trieste, 34127 Trieste, Italy

²³Department of Radiation Sciences, Uppsala University, 75121 Uppsala, Sweden

²⁴Department of Physics, University of Virginia, Charlottesville, Virginia 22901, USA

²⁵Sołtan Institute for Nuclear Studies and Warsaw University, 00681 Warsaw, Poland

²⁶Department of Physics, Yale University, New Haven, Connecticut 06511, USA

(Received 31 January 2004; published 23 July 2004)

We present a measurement of the longitudinal spin cross section asymmetry for deep-inelastic muon-nucleon interactions with two high transverse momentum hadrons in the final state. Two methods of event classification are used to increase the contribution of the photon-gluon fusion process to above 30%. The most effective one, based on a neural network approach, provides the asymmetries $A_p^{\ell N \rightarrow \ell h X} = 0.030 \pm 0.057(\text{stat}) \pm 0.010(\text{syst})$ and $A_d^{\ell N \rightarrow \ell h X} = 0.070 \pm 0.076(\text{stat}) \pm 0.010(\text{syst})$. From these values we derive an averaged gluon polarization $\Delta G/G = -0.20 \pm 0.28(\text{stat}) \pm 0.10(\text{syst})$ at an average fraction of nucleon momentum carried by gluons $\langle \eta \rangle = 0.07$.

I. INTRODUCTION

The Spin Muon Collaboration (SMC) has extensively studied polarized deep-inelastic lepton-nucleon scattering using the high energy muon beam at CERN and large targets containing polarized hydrogen and deuterium. The experimental study of the nucleon spin structure was pioneered in the 1970s [1]. The EMC experiment at CERN observed in the 1980s that only a small fraction of the proton spin is carried by the spin of the quarks [2]. The SMC results have confirmed this observation and have provided the first measurement of the spin structure of the deuteron which allowed for the verification of the fundamental Bjorken sum rule [3,4].

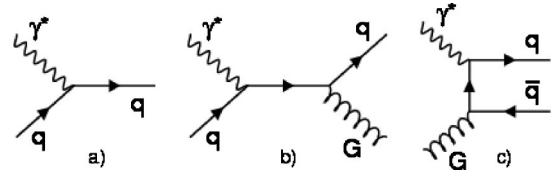


FIG. 1. Lowest order diagrams for DIS γ^* absorption: (a) leading process (LP), (b) gluon radiation (QCD-C), (c) photon-gluon fusion (PGF).

The high energy polarized data from SMC, combined with the high precision data from the SLAC [5] and DESY [6] experiments at lower energies, cover a kinematic range that allows for the analysis of the spin structure function g_1 in the framework of perturbative QCD. Various analyses have been performed at next-to-leading order, using different input parametrizations for the polarized parton densities and different choices for the fitted parameters [7,8]. They give consistent and precise results for the polarized quark densities, but have little sensitivity to the polarized gluon density ΔG . This is expected since g_1 is sensitive to gluons only through its evolution in Q^2 and since the available data on g_1 cover only a relatively narrow range in Q^2 at any given value of x . In particular, it is still not possible to test the hypothesis, formulated many years ago, that gluon spins may account for a sizable fraction of the nucleon spin [9].

A direct measurement of the gluon polarization is possible via the photon-gluon fusion (PGF) process, which is illustrated in Fig. 1, together with the two other leading order processes: virtual photon absorption [the leading process (LP)] and gluon radiation [QCD Compton scattering (QCD-C)]. Since the PGF contribution to the cross section is small, the event selection should be very effective in discriminating the PGF process from background. This can be achieved by selecting events in which either a charmed particle or hadrons of large transverse momenta (p_T) relative to the virtual photon direction are produced [10,11]. Both possibilities will be used in the COMPASS experiment at CERN [12], which is presently collecting data.

In this paper we present an evaluation of the polarization of the gluon inside the nucleon, $\Delta G/G$, from data by the SMC. We restrict the analysis to the deep-inelastic scattering (DIS) region ($Q^2 > 1 \text{ GeV}^2$) and select events with high p_T hadrons. The SMC experimental setup is not optimized for the detection of hadrons produced at large angles, so the precision of the present result is limited. This is, however, the first attempt to tag the PGF process with light quark production in a polarized DIS experiment.

A determination of the gluon polarization from events with high p_T hadrons has been attempted on the ep data from the HERMES experiment [13] at lower incident energy and in a kinematic range where quasireal photoproduction is dominant.

II. FORMALISM

The spin-dependent effects observed in experiments are generally small and have to be determined from the cross

*Deceased.

^aNow at CERN, 1211 Geneva 23, Switzerland.

^bNow at Texas Technical University, Lubbock, TX 79409-1051, USA.

^cNow at CIEMAT, Avda Complutense 22, 28040, Madrid, Spain.

^dNow at Fermi National Accelerator Laboratory, Batavia, IL 60510, USA.

^eNow at University of Wisconsin, USA.

^fNow at NIKHEF, 1009 AJ Amsterdam, The Netherlands.

^gNow at Bristol University, Bristol, UK.

^hNow at Brookhaven National Laboratory, Upton, NY 11973, USA.

ⁱNow at Dept. of Physics and Astronomy, SUNY at Stony Brook, Stony Brook, NY 11974, USA.

^jNow at Univ. of Illinois at Urbana-Champaign, 405 North Mathews Av. Urbana, IL 61801, USA.

^kPermanent address: Miyazaki University, Faculty of Engineering, 889-21 Miyazaki-Shi, Japan.

^lPermanent address: Paul Scherrer Institut, 5232 Villigen, Switzerland.

^mPermanent address: The Institute of Physical and Chemical Research (RIKEN), wako 351-01, Japan.

ⁿPermanent address: University of California, Institute of Particle Physics, Santa Cruz, CA 95064, USA.

^oPermanent address: KEK, Tsukuba-Shi, 305 Ibaraki-Ken, Japan.

^pNow at SBC Warburg Dillon Read, CH-4002 Basel, Switzerland.

^qNow at University of California, Department of Physics, Los Angeles, CA 90024, USA.

^rPermanent address: University of Buenos Aires, Physics Department, 1428 Buenos Aires, Argentina.

^sPermanent address: Rice University, Bonner Laboratory, Houston, TX 77251-1892, USA.

^tPermanent address: Warsaw University of Technology, 00-665 Warsaw, Poland.

^uNow at F.Hoffmann-La Roche Ltd., CH-4070 Basel, Switzerland.

^vNow at Oak Ridge National Laboratory, Oak Ridge, TN 37831-6393, USA.

^wNow at The Royal Library, 102 41 Stockholm, Sweden.

^xNow at Old Dominion University, Norfolk, VA 23529, USA.

^yNow at University of Bonn, 53115, Bonn, Germany.

^zNow at University of Illinois at Urbana-Champaign, USA.

^{aa}Now at SUBATECH, University of Nantes, UMR IN2P3/CNRS, 44307, Nantes, France.

^{ab}Now at Lawrence Berkeley National Laboratory, Berkeley, CA 94720, USA.

section asymmetry defined as the ratio of the polarized ($\Delta\sigma$) and unpolarized (σ) cross sections:

$$A^{\ell N} = \frac{\Delta\sigma}{2\sigma} = \frac{\sigma^{\uparrow\downarrow} - \sigma^{\uparrow\uparrow}}{\sigma^{\uparrow\downarrow} + \sigma^{\uparrow\uparrow}}, \quad (1)$$

where $\uparrow\downarrow$ and $\uparrow\uparrow$ refer to antiparallel and parallel spin configurations of the nucleon and the incoming lepton. At the parton level the hard-scattering cross section consists of three terms corresponding to the LP, QCD-C, and PGF processes. According to the factorization theorem, the cross sections σ and $\Delta\sigma$ can be written as convolutions of the parton distributions (F , ΔF), the hard-scattering cross sections ($\hat{\sigma}$, $\Delta\hat{\sigma}$), and the fragmentation functions (D) of partons into hadrons:

$$\begin{aligned} \sigma &= F \otimes \hat{\sigma} \otimes D, \\ \Delta\sigma &= \Delta F \otimes \Delta\hat{\sigma} \otimes D. \end{aligned} \quad (2)$$

The parton distributions refer to quarks, antiquarks, and gluons. The spin-dependent distributions are denoted by $\Delta q = q^\uparrow - q^\downarrow$ for quarks and antiquarks and by $\Delta G = G^\uparrow - G^\downarrow$ for gluons. The corresponding spin-averaged distributions are $q = q^\uparrow + q^\downarrow$ and $G = G^\uparrow + G^\downarrow$. Here, the up and down arrows indicate the relative configurations of the parton spin with respect to the nucleon spin.

When the full expressions for σ and $\Delta\sigma$ are inserted into Eq. (1), the expression for the cross section asymmetry for processes in which at least two hadrons with large transverse momenta are produced, $A^{\ell N \rightarrow \ell hhX}$, reads

$$\begin{aligned} A^{\ell N \rightarrow \ell hhX} &= \frac{\Delta q}{q} (\langle \hat{a}_{LL} \rangle^{LP} R_{LP} + \langle \hat{a}_{LL} \rangle^{QCD-C} R_{QCD-C}) \\ &+ \frac{\Delta G}{G} \langle \hat{a}_{LL} \rangle^{PGF} R_{PGF}, \end{aligned} \quad (3)$$

in which $\langle \hat{a}_{LL} \rangle = \langle \Delta\hat{\sigma}/2\hat{\sigma} \rangle$ is the average partonic asymmetry of a given process, and R is the ratio of its cross section for the given process with respect to the total cross section in the analyzed sample of events. A measurement of the asymmetry $A^{\ell N \rightarrow \ell hhX}$ thus permits the evaluation of the gluon polarization if all other contributions in Eq. (3) are known. The quark asymmetry $\Delta q/q$ is approximated by the value of the asymmetry A_1 obtained in inclusive measurements. The partonic asymmetries \hat{a}_{LL} are calculable and have been evaluated for simulated events in the kinematic region covered by the SMC data. On average they are positive for the LP and QCD-C processes and negative for the PGF process. The ratios R have been obtained from a sample of simulated events to which the same selection criteria have been applied as to the data.

The statistical precision of the gluon polarization determined from Eq. (3) depends on the precision of the measured asymmetry $A^{\ell N \rightarrow \ell hhX}$ and on the fraction of PGF events (R_{PGF}) in the final sample. Therefore, the aim of the present analysis is to select a large enough sample with a maximal contribution of PGF events.

The description of hadron production in muon DIS data in terms of the three processes of Fig. 1 has been successfully tested in previous experiments [14,15]. Other processes, such as those involving resolved photons, are expected to have small contributions for Q^2 above 1 GeV² and are not considered here.

III. EXPERIMENT

The experimental setup at the CERN muon beam consists of three major components: a polarized target, a magnetic spectrometer, and a muon beam polarimeter. A detailed description of the experiment and of the analysis of the inclusive data can be found in Refs. [4,16]. The muon beam polarization, P_B , has been determined from the spin asymmetries measured in polarized muon-electron scattering and from the energy spectrum of positrons from muon decays and found to be -0.795 ± 0.019 for an average beam energy of 187.4 GeV [17]. The target consists of two cells filled with butanol, deuterated butanol, or ammonia [18]. The target protons and deuterons are polarized in opposite directions for the two cells by dynamic nuclear polarization. The average target polarizations P_T are approximately 0.90 for protons and 0.50 for deuterons, with relative uncertainties $\Delta P_T/P_T$ of 3%–5%. The polarization was reversed 5 times a day during the data taking periods.

The counting rate asymmetry A^{expt} is determined from the number of events counted in the upstream and downstream target cells before and after the polarization reversals. This is done by solving a second order equation, as described in [19].

The cross section asymmetry $A^{\ell N \rightarrow \ell hhX}$ is related to A^{expt} by

$$A^{\ell N \rightarrow \ell hhX} = \frac{1}{P_B P_T f} A^{expt}, \quad (4)$$

where f is the effective dilution factor, which accounts for the dilution of the spin asymmetries by the presence of unpolarizable nuclei in the target and also for radiative effects on the polarized proton or deuteron. The effect of the unpolarizable materials can be expressed in terms of the numbers n_A of nuclei with mass number A and the corresponding total spin-independent cross sections σ_A^{tot} . The radiative effects on the proton or deuteron [16,20] are taken into account through the ratio of the one-photon-exchange cross section to the total cross section $\rho = \sigma_{p,d}^{1\gamma} / \sigma_{p,d}^{tot}$. The evaluation of the effective dilution factor for inclusive events and for events with observed hadrons is described in Ref. [4]. The asymmetries are corrected for radiative effects modifying the polarization as described in Refs. [16,21]. In the present analysis the polarized radiative corrections and the dilution due to radiative effects are reduced because processes without hadrons are excluded.

IV. SAMPLE SELECTION

The analysis uses the total sample of data collected by the SMC experiment during the years 1993–1996 with a muon

beam of $E = 190$ GeV and longitudinally polarized targets. The proton and deuteron samples have about the same size.

The standard SMC cuts on the inclusive kinematic variables [4], $\nu = E - E' > 15$ GeV and $E' > 19$ GeV, are imposed to reject events with poor kinematic resolution and muons from hadron decay, respectively. The cut $y = \nu/E < 0.9$ removes a region where the uncertainty due to radiative corrections is large. Two additional selections, closely related to the formalism used in the present analysis, are applied: A cut $Q^2 > 1$ GeV² rejects the region dominated by nonperturbative effects and allows one to interpret the results in terms of partons. A cut $y > 0.4$ removes events which carry little spin information owing to their small virtual photon polarizations. In addition, cuts on the muon scattering angle are applied to match the geometric acceptances of the hardware triggers.

Most hadrons in the LP have small transverse momenta p_T , which originate only from the intrinsic transverse momenta of quarks in the nucleon [22] and from the fragmentation mechanism. A different situation occurs for the QCD-C and PGF processes, where hadrons acquire transverse momenta mainly from primarily produced partons. For this reason, the requirement of two observed hadrons with large transverse momenta enhances the contribution of the PGF and QCD-C processes in the selected sample.

In the present analysis, the events of interest include a reconstructed incident muon, a scattered muon and at least two charged hadrons. They represent about 20% of the total number of events with a reconstructed beam and scattered muon used in the inclusive studies. Hadron tracks are accepted if they can be associated to the primary interaction point—i.e., the vertex—defined by the incoming and scattered muon tracks. The same association criteria as in the SMC analysis of Ref. [4] are applied. The contribution from the target fragmentation region is removed by cuts on the reduced longitudinal momentum of the hadron, $x_F > 0.1$, and on the hadron fractional energy, $z = E_h/\nu > 0.1$.

The further requirement of two hadrons with $p_T > 0.7$ GeV selects about 5% of the events passing all preceding selections. The contamination from electrons is expected to be negligible because electrons are generally produced at low p_T . This has been confirmed by examining the ratio of the energy deposited in the electromagnetic part of the calorimeter to the total deposited energy. No excess of events at 1.0 for tracks with $p_T > 0.5$ GeV was found. The total number of events after selections amounts to about 80 000 for the proton and 70 000 for the deuteron sample.

V. MONTE CARLO SIMULATION

A. Conditions for Monte Carlo generation

The interactions were simulated using the LEPTO 6.5 event generator [23] with a leading order parametrization of the unpolarized parton distributions [24]. The spin-dependent effects were calculated using POLDIS [25] with a consistent set of polarized parton distributions [26]. The kinematic limits of the Monte Carlo (MC) generation were defined so as to cover the full kinematic region of the data. Default values

were used for most of the steering parameters of the LEPTO generator. In the following we discuss only the modified conditions and parameters.

The matrix elements of first order QCD processes exhibit collinear divergences in the cross channel and different schemes are used to avoid such singularities. The so-called $z\hat{s}$ scheme, which allows for lower values of the γ^* -parton center-of-mass energy $\sqrt{\hat{s}}$, was used in the simulation with modified cutoff parameters. The effect of the cutoff values on any observable distribution for events with high p_T hadrons is marginal.

The description of interactions requires the choice of two scales: a factorization scale, which appears in the parton densities, and a renormalization scale, which appears in expressions depending on the strong coupling constant α_s . The usual choice of Q^2 was made for both scales. In these conditions, after kinematic cuts on event variables only, the generated sample contains 8% PGF events.

In order to describe the data, it was found necessary to change the values of two parameters describing the quark fragmentation in JETSET [27]. The function $f(z) = z^{-1}(1-z)^a e^{-bm_T^2/z}$, where $m_T^2 = m^2 + p_T^2$ and m is the mass of the quark, expresses the probability that a fraction z of the available energy will be carried away by a newly created hadron. The parameters (a, b) were modified from their default values $(0.3, 0.58)$ to $(0.5, 0.1)$, a change making the fragmentation softer. This modification was inspired by a similar study done by the HERMES experiment [28,29]. It appears to work also in the present case, with smaller deviations from the default values. We note, however, that we consider here a particular sample of events and that we have no possibility to verify if a Monte Carlo sample generated with these modifications would correctly describe the full data. The uncertainty associated with these modifications has been estimated and is included in the systematic error.

B. Simulation of experimental conditions

The scattered muon track of each simulated event has been traced through the magnet aperture. The trigger conditions have been checked and prescaling factors have been applied to reproduce the relative trigger rates of the experiment in the simulated sample. The kinematic parameters of the muon and hadron tracks and the coordinates of the vertex position have been smeared according to the experimental resolution. In addition, the loss of tracks due to detector inefficiencies is taken into account by applying detection plane inefficiencies to the simulated events and by removing the tracks which do not longer fulfill the minimal requirements for reconstruction.

Secondary interactions of hadrons have to be taken into account to reproduce the distribution of interaction vertices along the target axis. Hadrons have been rejected from the sample according to the probability of reinteraction in the polarized target material. As an example, Fig. 2 shows the agreement obtained for the vertex position along the beam axis in one of the proton data sets.

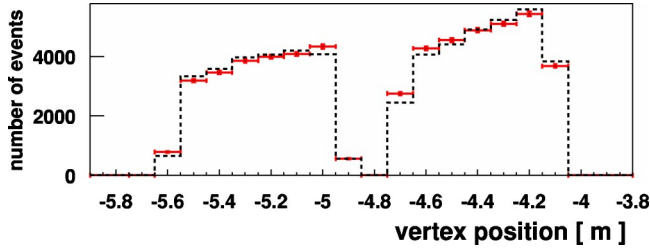


FIG. 2. The distribution of vertices along the beam axis. The points correspond to the proton data from 1993 and the histogram to the corresponding Monte Carlo simulation.

The simulation has been performed separately for each year of data taking. To obtain a good description of the kinematic variables it is necessary to use specific beam parameters for every year, including small changes in angles, and to take into account the exact target position.

C. Comparison of simulations and data

The distributions of kinematic variables as well as the particle distributions in the detectors have been checked with identical selection criteria applied to the data and to the simulated events. For the latter, cuts have been applied to the smeared variables. The distributions of x and Q^2 for interactions on protons are presented in Fig. 3. The obtained agreement is at the level of 10%–25% for all kinematic event variables. The level of agreement for deuterons is very similar [30].

The same comparisons have been made for the hadron observables. Clear discrepancies have been found in simulations performed with the unmodified fragmentation function for the hadron production angle θ and the longitudinal momentum p_L , while satisfactory agreement has been obtained for p_T , except at the highest values. The observed differences at the highest values of p_T can be explained by the approximate description of the non-Gaussian tails of the dis-

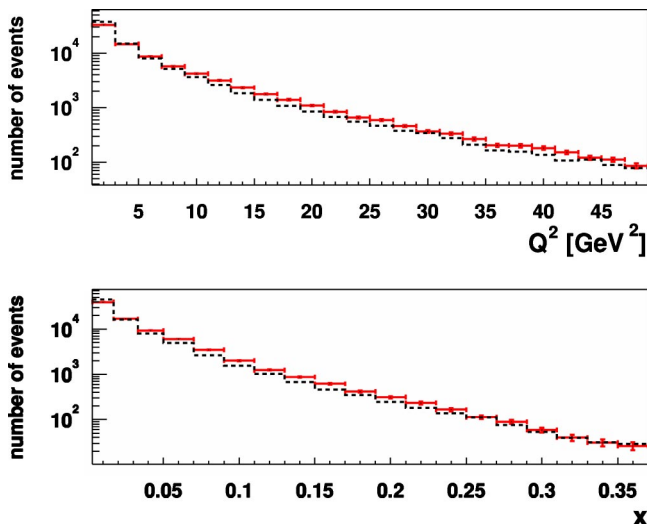


FIG. 3. The x and Q^2 distributions for the proton data: the points correspond to the data and the histograms to the Monte Carlo simulation normalized to the same number of events.

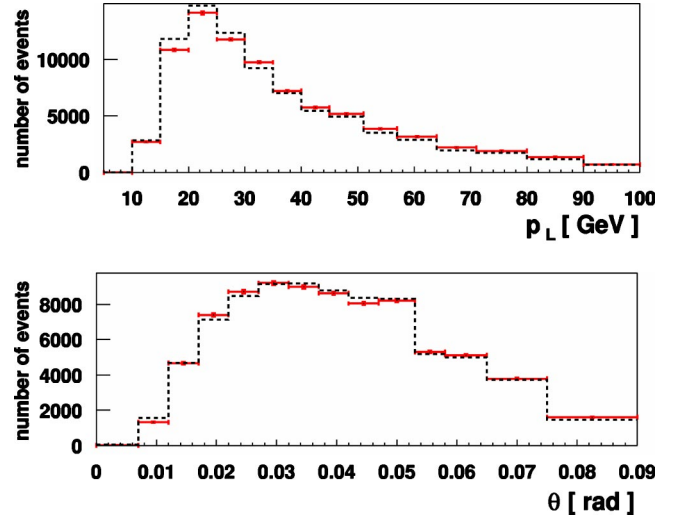


FIG. 4. The distributions of the longitudinal momentum and the scattering angle for the hadron with the highest p_T . The points correspond to the proton data from 1993 and the histograms to the Monte Carlo simulation with the modified fragmentation function.

tributions used for smearing and by the effects of real photon radiation, which are not taken into account in the present analysis. It has been checked that the discrepancy for the θ angle cannot be removed by using different smearing parametrizations or even by an artificial increase of the smearing. Agreement between data and simulation can be achieved only by applying an *ad hoc* cut on the hadron production angle $\theta > 0.02$ rad. This cut, however, removes about 25% of the selected sample and cannot be justified since there is no reason why the simulation should fail to describe hadrons produced at low θ . Therefore, modified simulation conditions providing a better description of the data have been searched for.

When the parameters of the fragmentation function are modified (cf. Sec. V A), the agreement becomes satisfactory over a wide range in p_L and θ . The comparison of the p_L and θ distributions is shown in Fig. 4 for the hadron with highest p_T . Also the second hadron is well described by the simulation [30]. We conclude that the parameters of the longitudinal fragmentation function $f(z)$ have to be modified to obtain a good description of the data over the full range of the hadron production angle θ . Since it is difficult to check if the modified set of parameters correctly describes the semi-inclusive hadron distributions, the analysis has been performed with the modified fragmentation as well as with the standard fragmentation and an additional cut on $\theta > 0.02$ rad.

VI. SELECTION OF THE PGF PROCESS

In order to compare the merits of various selections of PGF events, we define the *efficiency* ϵ , which is the fraction of PGF events accepted by the selection criteria, and the *purity* R_{PGF} [Eq. (3)], which is the ratio of the number of selected PGF events to the total number of selected events. The optimal selection is obviously the one providing the highest values of ϵ and R_{PGF} but, in general, an increase of

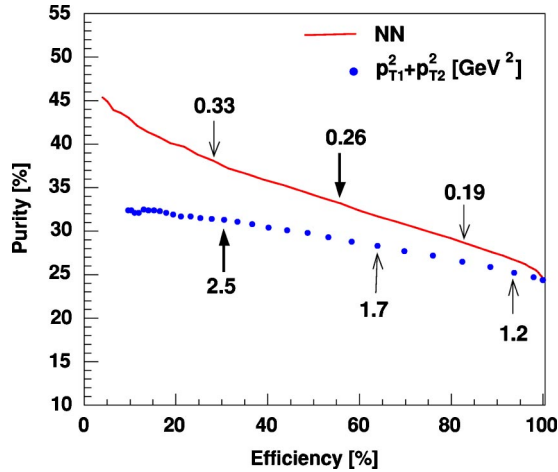


FIG. 5. The purity and efficiency obtained in the selection of the PGF process with the methods based on the NN response (solid curve) and the cut on Σp_T^2 (points), applied to simulated events. The numbers give the values of NN thresholds and the values (in GeV^2) of the applied cuts on Σp_T^2 corresponding to the purity-efficiency points indicated by the arrows. The simulations correspond to the proton data sample.

the former will result in a decrease of the latter.

The purity is 0.11 for the full sample of events with at least two charged hadrons. The additional requirement of two hadrons with $p_T > 0.7$ GeV defines our reference sample for which $R_{PGF} = 0.24$ and, by convention, $\epsilon = 1$.

The effects of cuts have been studied for the following variables: p_{T1} , the sum $p_{T1}^2 + p_{T2}^2$, the hadron charges (same or opposite sign), the azimuthal angle ϕ between the momenta of the two hadrons with respect to the virtual photon direction, and the invariant mass of the two hadrons (see also Ref. [31]). It was found that the selection on Σp_T^2 is optimal for enhancing the PGF purity and that further requirements on the hadron charges do not yield significant improvement. Figure 5 shows the variation of R_{PGF} with ϵ when the cut on Σp_T^2 is varied up to 4 GeV^2 . It is seen that the purity increases only very slowly when the cut is made more restrictive while the efficiency drops very rapidly. This can be understood by the fact that the QCD-C background process has a similar dependence on the Σp_T^2 cut as the PGF process. The use of A_1 for the quark asymmetry in Eq. (3) is valid only if the fraction of PGF events in the selected sample is much higher than in the inclusive sample—i.e., close to the maximum value of 0.33. In addition, the efficiency needs to be sufficiently high to allow a meaningful analysis. As a compromise, we have fixed the cut on p_T^2 at 2.5 GeV^2 , which corresponds to $\epsilon = 0.30$ and $R_{PGF} = 0.31$.

The combination of several variables into a single parameter has been investigated in a classification procedure based on a neural network (NN) [30,32]. We consider the variables which characterize the DIS event (x , Q^2 , y , and the multiplicity of tracks) and those which describe the two selected hadrons with highest p_T (the transverse and longitudinal hadron momenta, the charges of the hadrons, the energy fractions of the hadrons, and the azimuthal angle ϕ). The classification procedure is trained on a Monte Carlo sample

where the actual process is known for each event. As a result, the procedure provides a single value, called “NN response,” within the range (0,1). High values of this response correspond to events which, according to the classification algorithm, are more likely to result from PGF than from background processes. A threshold on the network response can thus be used to select a PGF enriched sample.

The variation of R_{PGF} vs ϵ for various choices of the NN response threshold is shown in Fig. 5. It is seen that at equal efficiency the NN approach always provides samples with higher purity than the approach based on Σp_T^2 selection. For further analysis, a threshold of 0.26 has been chosen, which corresponds to $R_{PGF} = 0.33$ and $\epsilon = 0.56$. A similar purity is obtained with the Σp_T^2 cut at 2.5 GeV^2 but with a lower efficiency of 30%. Therefore, a better statistical precision on the measured asymmetry is obtained with the NN method. Alternatively, a higher NN threshold corresponding to a PGF efficiency of 30% would yield a sample where the purity is about 37%—i.e., 6% higher than the value obtained with the Σp_T^2 cut. The comparison of the two selected samples shows that the NN procedure selects a large fraction of events with $\Sigma p_T^2 > 2.5$ GeV^2 but also covers the lower range of Σp_T^2 . It has been checked that the distributions of NN responses are compatible for data and Monte Carlo events.

VII. SPIN ASYMMETRIES $A^{\ell N \rightarrow \ell h h X}$

The SMC data taken from 1993 to 1996 have been split into periods of data taking, each containing about 15 days. The asymmetry for a given year is the weighted average of the asymmetries calculated for each period of data taking. Splitting the data into smaller subsamples gives identical results within the expected statistical fluctuations. The distribution of the vertex position along the beam axis, as presented in Fig. 2, shows that the ratio of acceptances for the upstream to downstream target cells is about 0.7. The method used for asymmetry calculation, described in [19], is suited for such an acceptance difference.

The asymmetry has been calculated for the entire sample, which has a purity $R_{PGF} = 0.24$, and for the two selection methods with enhanced R_{PGF} ($\Sigma p_T^2 > 2.5$ GeV^2 and NN response > 0.26). The results given in Fig. 6 and Table I show that the asymmetries do not change significantly with the selection. The asymmetries obtained for the proton and for the deuteron are compatible within the errors. The statistical uncertainty is larger for the selection based on Σp_T^2 because a smaller fraction of events is selected (28% vs 42%).

The uncertainties in the measured $A^{\ell N \rightarrow \ell h h X}$ asymmetry for the selected samples are dominated by statistics. The contributions to the systematic uncertainty on $A^{\ell N \rightarrow \ell h h X}$ are detailed in Table II for the two selections with enhanced R_{PGF} . The most significant systematic uncertainties arise from the false asymmetries, the fraction of radiative processes (ρ), and the polarized radiative corrections. For the false asymmetries an upper limit from the time variation of the acceptance has been evaluated under the assumption that the reconstruction for each of the three tracks (the scattered muon and the two hadrons) is affected independently. The method

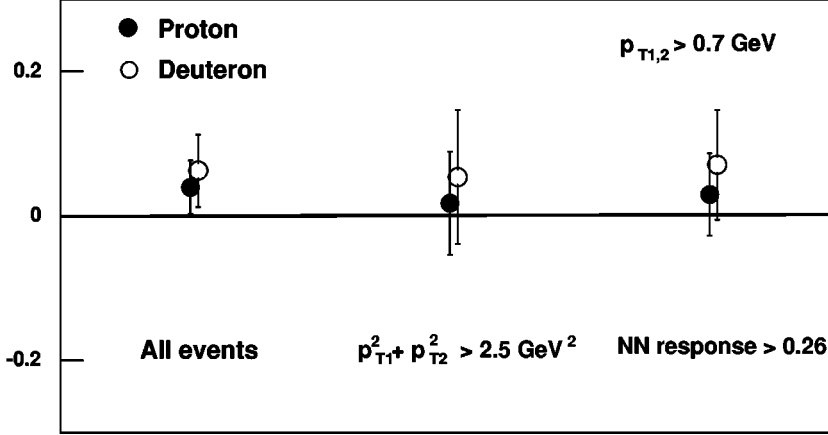
$A^{\ell N \rightarrow \ell h h X}$


FIG. 6. The measured asymmetry $A^{\ell N \rightarrow \ell h h X}$, for the proton and the deuteron, for events with $p_{T1,2} > 0.7$ GeV cut (left) and after the additional selection on Σp_T^2 (center) or on the NN response (right). The errors are predominantly statistical.

used for estimating these effects is described in Ref. [31]. The radiative corrections are small due to the limited phase space available for real photon emission in the events where a significant fraction of the available energy is taken by the two hadrons with large p_T . The uncertainties in ρ and in the polarized radiative corrections were taken equal to the full size of the inelastic contribution. The effect of real photon radiation on the event kinematics and, in particular, on the value of p_T itself has not been taken into account in view of the limited precision of the present data.

VIII. DETERMINATION OF THE GLUON POLARIZATION

The gluon polarization is evaluated from Eq. (3) using the measured $A^{\ell N \rightarrow \ell h h X}$ asymmetry, obtained for the samples with enhanced R_{PGF} , quoted in Table I. In view of the strong dependence of the resulting gluon polarization on the information obtained from the Monte Carlo simulation, special attention must be given to the consistency of data and simulated events. The level of the agreement reached can be judged by comparing the distributions shown in Figs. 2–4.

The quark polarization entering in the first term on the right-hand side of Eq. (3) is approximated by the average value of the inclusive asymmetry $A_1(x)$ for the full proton and deuteron samples. The average is computed using the parametrization of $A_1(x)$ from the fit to all existing data and the x value of every selected event.

The partonic asymmetries \hat{a}_{LL} for each of the subprocesses are calculated for each Monte Carlo event and are averaged. The values for LP and QCD-C are very similar for

TABLE I. The measured cross section asymmetries $A^{\ell N \rightarrow \ell h h X}$ for the proton and deuteron data with $p_{T1,2} > 0.7$ GeV, with the sample with $\Sigma p_T^2 > 2.5$ GeV², and with the NN response > 0.26 . The first uncertainty is statistical and the second is systematic.

Selection	$A_p^{\ell N \rightarrow \ell h h X}$	$A_d^{\ell N \rightarrow \ell h h X}$
All	$0.041 \pm 0.037 \pm 0.011$	$0.063 \pm 0.050 \pm 0.011$
$\Sigma p_T^2 > 2.5$ GeV ²	$0.018 \pm 0.071 \pm 0.010$	$0.054 \pm 0.093 \pm 0.008$
NN response > 0.26	$0.030 \pm 0.057 \pm 0.010$	$0.070 \pm 0.076 \pm 0.010$

the Σp_T^2 cut and the NN selection, $\langle \hat{a}_{LL} \rangle^{LP} = 0.8$ and $\langle \hat{a}_{LL} \rangle^{QCD-C} = 0.6$, on average. The value of $\langle \hat{a}_{LL} \rangle^{PGF}$ is -0.44 and -0.49 for the Σp_T^2 cut and the NN selection, respectively.

The values of the ratios R provided by the simulation for the LP, QCD-C, and PGF processes are 0.26, 0.43, and 0.31 for the selection on Σp_T^2 and 0.38, 0.29, and 0.33 for the NN selection. The contributions of the different processes for the proton and deuteron samples differ by less than 0.02.

The gluon polarization is determined for the kinematic region covered by the selected sample and corresponds to a fraction η of nucleon momentum carried by the gluon given by

$$\eta = x \left(\frac{\hat{s}}{Q^2} + 1 \right). \quad (5)$$

This quantity is known for simulated events but cannot be directly determined from the data. Nevertheless, \hat{s} can be approximately calculated from the virtual photon energy in

TABLE II. The contributions to the systematic error of $A^{\ell N \rightarrow \ell h h X}$ with the $\Sigma p_T^2 > 2.5$ GeV² cut and with the NN response > 0.26 for the proton and deuteron data. The first and last contributions are additive; the others are proportional to the asymmetry.

Contributions to the systematic error on $A^{\ell N \rightarrow \ell h h X}$	Proton data		Deuteron data	
	Σp_T^2	NN	Σp_T^2	NN
False asymmetries	0.0049	0.0049	0.0044	0.0044
Target polarization	0.0005	0.0008	0.0016	0.0023
Beam polarization	0.0007	0.0011	0.0021	0.0029
Dilution factor				
Target composition	0.0003	0.0001	0.0002	0.0001
ρ factor	0.0018	0.0030	0.0054	0.0076
Polarized rad. corr.	0.0083	0.0083	0.0020	0.0020
Total systematic error	0.0098	0.0102	0.0077	0.0097

TABLE III. The gluon polarization for the proton and the deuteron data from the analyzed sample with $\Sigma p_T^2 > 2.5 \text{ GeV}^2$ and with the NN response > 0.26 . The first uncertainty is statistical and the second is systematic.

Selection	$(\Delta G/G)_p$	$(\Delta G/G)_d$	$\langle \eta \rangle$
$\Sigma p_T^2 > 2.5 \text{ GeV}^2$	$0.11 \pm 0.51 \pm 0.12$	$-0.37 \pm 0.66 \pm 0.12$	0.09
NN response > 0.26	$-0.06 \pm 0.35 \pm 0.10$	$-0.47 \pm 0.49 \pm 0.10$	0.07

the laboratory system and from the angles (θ_1, θ_2) defined by the directions of the two hadrons with respect to the virtual photon:

$$\hat{s} \approx \nu^2 \tan(\theta_1) \tan(\theta_2). \quad (6)$$

To check the validity of this approximation in our kinematic conditions, we have compared the generated η and the one calculated from the above equation for selected PGF events. The calculated values are on average 25% higher than the generated ones. The averaged value of the generated η for the selected PGF events in the Monte Carlo simulation is used as the reference value for the result on $\Delta G/G$. We have also checked the average values of η calculated for all simulated events and obtained the values 0.15 for the cut $\Sigma p_T^2 > 2.5 \text{ GeV}^2$ and 0.10 for the NN response > 0.26 . For both selection methods the values of η calculated for all simulated events and for the data are very close. The results on the gluon polarization and the values of $\langle \eta \rangle$ are presented in Table III.

In addition to the systematic errors on the measured asymmetry discussed in Sec. VII and given in Table II, the asymmetry A_1 , the fractions R , and the partonic asymmetries $\langle \hat{a}_{LL} \rangle$ contribute to the systematic error in $\Delta G/G$. The contribution due to the asymmetry A_1 is determined from the uncertainty in A_1 at the averaged value of x and thus from the errors on the fit parameters. The value of A_1 at the average x agrees with the average A_1 calculated from the fit for each event to within 0.001.

The dominant contributions to the systematic error are due to the uncertainties on the values of R and $\langle \hat{a}_{LL} \rangle$. They are estimated by comparing the results obtained from Monte Carlo simulations with different parameters. For this purpose, a sample of LEPTO events was generated with the same kinematic and hadron selections but with modified renormalization and factorization scales, cutoffs, and fragmentation function parameters. Scales of $Q^2/2$ and $2 Q^2$ are used for comparison and provide an estimate of the stability of the leading order approximation used here. Results with standard and modified parameters (see Sec. V A) in the fragmentation function were compared. Since only the simulations which reproduce the data should be considered, a cut on the hadron angle θ is applied, as explained in Sec. V C. The value of the gluon polarization calculated with this new Monte Carlo sample was compared to the one obtained under the conditions described in Sec. V A. This procedure was repeated several times with slightly different cuts and with different NN thresholds. For the NN approach a complica-

TABLE IV. The contributions to the systematic error on the gluon polarization for the $\Sigma p_T^2 > 2.5 \text{ GeV}^2$ cut and for the NN response > 0.26 .

Source of the uncertainty	Σp_T^2	NN
Systematic error on $A^{\ell N \rightarrow \ell h h X}$	0.072(p) 0.057(d)	0.061(p) 0.063(d)
Precision of A_1 fit	0.042(p) 0.042(d)	0.026(p) 0.028(d)
Scale change from $Q^2/2$ to $2 Q^2$	0.008	0.010
Fragmentation parameters	0.036	0.034
Cutoffs in matrix elem.	0.015	0.008

tion arises from the fact that any change in the simulation procedure leads to a different selection on the data. To avoid the fluctuation of the gluon polarization due to a variation of the measured asymmetry, the value of this asymmetry has been artificially frozen when comparing results for different Monte Carlo samples. The individual contributions to the systematic error are given, for both selection methods, in Table IV. It has been checked that the effect of combined modifications in the Monte Carlo simulations is smaller than the sum of the individual uncertainties. The maximal variation of R_{PGF} and $\langle \hat{a}_{LL} \rangle$ is found to be 20% and 4%, respectively.

As discussed before, the NN selection provides a more accurate result than the selection based on Σp_T^2 cuts. The statistical error is, however, too large to draw definitive conclusions on the contribution of ΔG to the nucleon spin. The systematic uncertainty is small compared to the statistical error. The demand of good agreement between the simulation and the data forms an important limitation in estimating the systematic uncertainties. For this reason, an increase in statistical precision is expected to lead to further improved systematic uncertainty estimates.

By averaging the results for the proton and the deuteron obtained with the neural network classification we obtain $\Delta G/G = -0.20 \pm 0.28$ (stat) ± 0.10 (syst).

IX. CONCLUSIONS

We have evaluated for the first time the gluon polarization from the spin asymmetries measured in lepton-nucleon DIS events with $Q^2 > 1 \text{ GeV}^2$ including two hadrons with large transverse momentum in the final state. The analysis is performed at leading order in QCD and is based on the comparison of selected data samples with simulated events provided by the LEPTO generator. The partonic asymmetry \hat{a}_{LL} is mostly negative for the photon-gluon fusion process while it is positive for the two competing processes: the leading process and gluon radiation. The relative contribution of photon-gluon fusion is enhanced to about 30% by applying a cut on $\Sigma p_T^2 > 2.5 \text{ GeV}^2$ or by using a neural network classification.

The average gluon polarization obtained for the SMC data is close to zero with a large statistical error (~ 0.30). The precision is limited by the reduction of the analyzed event

sample to less than 1% of the DIS sample by the hadron selection requirements. It is thus expected to be improved by higher counting rates and a larger hadron acceptance in on-going and future experiments.

ACKNOWLEDGMENTS

This work was supported by Bundesministerium für Bildung, Wissenschaft, Forschung und Technologie, partially supported by TUBITAK and the Center for Turkish-Balkan Physics Research and Application (Bogziçi University), sup-

ported by the U.S. Department of Energy, the U.S. National Science Foundation, Monbusho Grant-in-Aid for Science Research (International Scientific Research Program and Specially Promoted Research), the National Science Foundation (NWO) of the Netherlands, the Commissariat à l'Énergie Atomique, Comision Interministerial de Ciencia y Tecnología and Xunta de Galicia, the Israel Science Foundation, and Polish State Committee for Scientific Research (KBN) SPUB No. 134/E-365/SPUB-M/CERN/P-03/DZ299/2000 and 621/E-78/SPB/CERN/P-03/DWM 576/2003-2006 and Grant No. 2/P03B/10725.

-
- [1] V.W. Hughes, Nucl. Phys. **A518**, 371 (1990).
 [2] EMC, J. Ashman *et al.*, Nucl. Phys. **B328**, 1 (1989); Phys. Lett. B **206**, 364 (1988).
 [3] SMC, B. Adeva *et al.*, Phys. Lett. B **302**, 533 (1993).
 [4] SMC, B. Adeva *et al.*, Phys. Rev. D **58**, 112001 (1998).
 [5] E142, P.L. Anthony *et al.*, Phys. Rev. D **54**, 6620 (1996); E143, K. Abe *et al.*, Phys. Rev. D **58**, 112003 (1998); E154, K. Abe *et al.*, Phys. Rev. Lett. **79**, 26 (1997); E155, P.L. Anthony *et al.*, Phys. Lett. B **458**, 529 (1999).
 [6] HERMES, A. Airapetian *et al.*, Phys. Lett. B **442**, 484 (1998).
 [7] SMC, B. Adeva *et al.*, Phys. Rev. D **58**, 112002 (1998); E155, P.L. Anthony *et al.*, Phys. Lett. B **493**, 19 (2000).
 [8] G. Altarelli, R.D. Ball, S. Forte, and G. Ridolfi, Nucl. Phys. **B496**, 337 (1997); E. Leader, A.V. Sidorov, and D.B. Stamenov, Eur. Phys. J. C **23**, 479 (2002); Y. Goto *et al.*, Phys. Rev. D **62**, 034017 (2000); M. Glück, E. Reya, M. Stratmann, and W. Vogelsang, *ibid.* **63**, 094005 (2001); J. Blümlein and H. Bottcher, Nucl. Phys. **B636**, 225 (2002); C. Bourrely, J. Soffer, and F. Buccella, Eur. Phys. J. C **23**, 487 (2002).
 [9] A.V. Efremov and O.V. Teryaev, JINR Report No. E2-88-287, Dubna, 1988; G. Altarelli and G.G. Ross, Phys. Lett. B **212**, 391 (1988); P.G. Ratcliffe, *ibid.* **192**, 180 (1987).
 [10] R.D. Carlitz, J.C. Collins, and A.H. Mueller, Phys. Lett. B **214**, 229 (1988).
 [11] A. Bravar, D. von Harrach, and A. Kotzinian, Phys. Lett. B **421**, 349 (1998).
 [12] COMPASS, G. Baum *et al.*, "COMPASS: A Proposal for a Common Muon and Proton Apparatus for Structure and Spectroscopy," Report No. CERN-SPSLC-96-14.
 [13] HERMES, A. Airapetian *et al.*, Phys. Rev. Lett. **84**, 2584 (2000).
 [14] EMC, M. Arneodo *et al.*, Phys. Lett. **149B**, 415 (1984); Z. Phys. C **36**, 527 (1987).
 [15] E665, M.R. Adams *et al.*, Phys. Rev. D **48**, 5057 (1993); Phys. Rev. Lett. **72**, 466 (1994).
 [16] SMC, D. Adams *et al.*, Phys. Rev. D **56**, 5330 (1997).
 [17] SMC, B. Adeva *et al.*, Nucl. Instrum. Methods Phys. Res. A **443**, 1 (2000).
 [18] SMC, B. Adeva *et al.*, Nucl. Instrum. Methods Phys. Res. A **437**, 23 (1999).
 [19] L. Klosterman, Ph.D. thesis, Delft University of Technology, Delft, 1995.
 [20] A.A. Akhundov *et al.*, Fortschr. Phys. **44**, 373 (1996); Sov. J. Nucl. Phys. **26**, 660 (1977); **44**, 988 (1986); D. Bardin and N. Shumeiko, *ibid.* **29**, 499 (1979).
 [21] T.V. Kukhto and N.M. Shumeiko, Nucl. Phys. **B219**, 412 (1983).
 [22] A. König, Z. Phys. C **18**, 63 (1983).
 [23] G. Ingelman, A. Edin, and J. Rathsmann, Comput. Phys. Commun. **101**, 108 (1997).
 [24] M. Glück, E. Reya, and A. Vogt, Z. Phys. C **67**, 433 (1995).
 [25] A. Bravar, K. Kurek, and R. Windmolders, Comput. Phys. Commun. **105**, 42 (1997).
 [26] T. Gehrmann and W.J. Stirling, Phys. Rev. D **53**, 6100 (1996).
 [27] T. Sjöstrand *et al.*, Comput. Phys. Commun. **135**, 238 (2001).
 [28] HERMES, N.C.R. Makins (private communication).
 [29] P. Geiger, Ph.D. thesis, University of Heidelberg, 1998.
 [30] K. Kowalik, Ph.D. thesis, Institute for Nuclear Studies, Warsaw, 2004.
 [31] H. Gilly, Ph.D. thesis, University of Freiburg, 2000.
 [32] K. Kowalik *et al.*, Acta Phys. Pol. B **32**, 2929 (2001).